Article

SHM Structural Health Monitoring

Structural Health Monitoring
11(3) 359–366
© The Author(s) 2011
Reprints and permissions:
sagepub.co.uk/journalsPermissions.nav
DOI: 10.1177/1475921711419992
shm.sagepub.com

SAGE

The influence of propagation path on elastic waves as measured by acoustic emission parameters

DG Aggelis[1], T Shiotani[2], A Papacharalampopoulos[3] and D Polyzos[3]

Abstract

Apart from the quantitative parameters of acoustic emission testing, such as the total activity or the location of the sources, much more information can be exploited by qualitative characteristics of the signals. The shape of the waveform strongly depends on the source, supplying information on the type of cracks. Shear cracks which normally follow tensile during fracture, emit signals with longer rise time as well as lower average frequency. However, due to the inherent inhomogeneity of the media, which is enhanced by the nucleation of cracks, each pulse suffers strong dispersion which results in serious alteration of the waveform shape. Therefore, classification of cracks based on acoustic emission parameters would be probably misleading in case the separation distance of the sensors is long or the material contains many cracks. In the present study, numerical simulations were conducted in order to examine the influence of distance on the shape distortion of an excited wave inside concrete. Results are compared with actual experiments on steel fiber reinforced concrete, showing that the distance between the source crack and the acquisition point should not exceed a threshold value in order to lead to reliable crack classification.

Keywords

concrete, health monitoring, heterogeneity, frequency, RA, scattering, simulation, wave propagation

Introduction

Acoustic emission (AE) is a method widely used for real time monitoring of the structural condition of different materials and structures. It is based on the elastic energy which is released during changes in the material structure, such as crack nucleation and propagation, changes in microstructure, etc. This energy is transmitted through the material in the form of transient elastic waves and can be detected by appropriate sensors on the surface of the material.[1,2] Typically, the accumulated activity recorded by the sensors is indicative of the severity of cracking, since the existence of cracks is usually the prerequisite for AE generation; high AE rate of incoming signals indicates the existence of many active cracks while low or no emissions denote sound material. Certain indices based on the magnitude or the number of the AE signals have been employed successfully in the health monitoring of structural materials like concrete.[3,4] When multiple sensors are applied, apart from the number of AE hits, significant information concerning the location of the source events can be derived based on the time delay between acquisition of the corresponding signals at different sensors.[5,6] This allows estimation of which part of the material needs repair which is of paramount importance for large scale structures.

However, there are other important aspects of the AE testing, which are based on the qualitative parameters of the received signals. It has been seen that the shape of the waveforms is indicative of the fracture type, something

[1]Department of Materials Science and Engineering, University of Ioannina, Greece.
[2]Graduate School of Engineering, Kyoto University, Nishikyo-ku, Kyoto 615-8540, Japan.
[3]Department of Mechanical Engineering and Aeronautics, University of Patras, Greece.

Corresponding author:
D.G. Aggelis, Department of Materials Science and Engineering, University of Ioannina, Greece
Email: daggelis@cc.uoi.gr

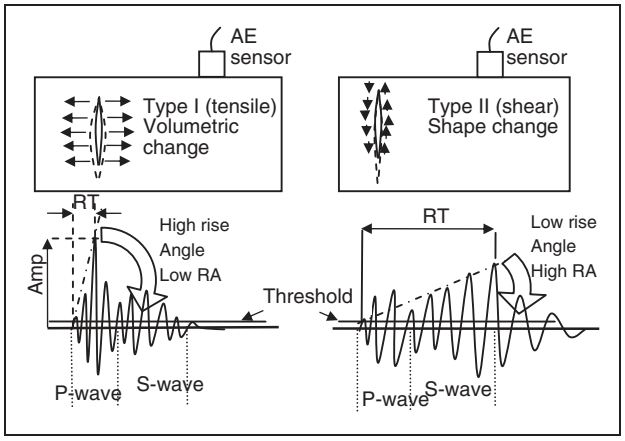

Figure 1. Cracking modes and corresponding AE signals.

very important for the classification of cracks in different materials.[7–9] In general shear cracks follow tensile as the material fails. Therefore, the characterization of the cracking mode can act as a precaution against final failure. It can simply be stated that when a tensile event occurs, the sides of the crack move away from each other. This motion leads to a transient volumetric change in the material. Therefore, most of the energy is released in the form of longitudinal (dilatational waves) and only a small amount in the form of S-waves which are slower. Consequently, the major part of energy arrives quite early within the waveform.[10] Figure 1 (left) shows a schematic representation of AE waveform emitted by a tensile event. The delay between the onset and the highest peak, denoted as Rise time (RT) is quite short, leading to high Rise Angle. On the other hand a shear cracking event (seen on the right of Figure 1) causes mainly shape deformation which emits most of the energy in S-waves and only a small amount of energy in the form of longitudinal. Therefore, the major part of energy (maximum amplitude) arrives much later than the initial disturbance of the longitudinal wave which is faster, leading to longer RT and consecutively lower Rise Angle, as seen on the right of Figure 1. Recently the shape of the initial part of the waveform is quantified by the RA value (RT over maximum Amplitude) and is measured in μs/V, as proposed by the relevant recommendations.[11] Additionally, tensile events exhibit higher frequency characteristics than shear, as expressed by the Average Frequency (AF), which is the number of threshold crossings over the duration of the signal.[11] It is mentioned that in AE measurements a minimum voltage is required in order to trigger the acquisition. This is called 'threshold' and it is defined in such a way to exclude low ambient noise from being recorded.

This kind of classification has proved very useful concerning corrosion cracking in concrete,[8] rock failure,[9] fracture of cross-ply laminates,[7,12] discrimination between tensile matrix cracking, and fiber pull-out during bending of steel fiber reinforced concrete (SFRC),[13,14] as well as damage monitoring during seismic loading of reinforced concrete frames.[15]

However, it should be kept in mind that the AE signals are transient elastic waves, the propagation of which depends on the distance and the quality of the path. Specifically, when a pulse propagates in a heterogeneous medium, apart from the attenuation, it also suffers dispersion or shape distortion.[16] This has been experimentally measured in different systems that contain phases with strong impedance mis-match[17,18] and it is mainly attributed to scattering,[19] which redirects the wave beam and therefore, alters the arrival time of some wave components. The shape of the waveform will change depending on the heterogeneity of the path, either due to the constituent phases, if a composite material is examined, or/and due to the existence of cracks.[20] Guided waves, such as those found in thin shell-type structures, can have similar effect upon waveform shape.[21,22] Since the shape of the wave changes, it is expected that the calculation of AE parameters will be affected. This practically means that one specific event will be recorded as having different waveform shapes for sensors placed at close or further distances from the source. Therefore, the influence of the distance in the measurement of AE parameters should be studied especially in relation with standardization which is currently being attempted for the field of concrete.[11,23]

In this article, the relation between the measured AE parameters and the propagation distance through concrete is numerically studied. The simulations concern elastic matrix with stiff aggregates in order to resemble concrete, while the influence of cracks is also studied. It is shown that the separation distance of the sensors is of paramount importance and it should be taken into account when crack mode estimation is attempted by data from in-situ monitoring projects.

Numerical simulation

The fundamental equation governing the two-dimensional propagation of stress waves in an elastic medium, with viscous losses is as follows:

$$\rho\frac{\partial^2 u}{\partial t^2}=\left(\mu+\eta\frac{\partial}{\partial t}\right)\nabla^2 u+\left(\lambda+\mu+\xi\frac{\partial}{\partial t}+\frac{n}{3}\frac{\partial}{\partial t}\right)\nabla\nabla\cdot u \quad (1)$$

where u=u(x,y,t) is the time-varying displacement vector, ρ is the mass density, λ and μ are the first and second Lame constants, η and ξ are the first and second viscosities respectively, and t is time. The simulations were conducted using commercially available

software.[24] It operates by solving the above equation based on the method of finite differences. Equation (1) is solved with respect to the boundary conditions of the model, which include the input source that has predefined time-dependent displacements at a given location and a set of initial conditions.[25] For heterogeneous media like the one studied herein, wave propagation in each distinct homogeneous phase (in this case mortar matrix and aggregates) is solved according to Equation (1), while the continuity conditions for stresses and strains must be satisfied on the interfaces.[25]

The materials were considered elastic with damping. The numerical model included the mortar matrix, round aggregates, and in most cases cracks, simulated by thin films. The corresponding properties of the materials used in the model can be seen in Table 1. Since data on the equivalent viscosity of concrete were not available, parameters were fitted in order to match attenuation from relevant experiments in cement materials.[26] The material used for the cracks was assigned properties of air, while no viscosity was included, see again Table 1.

In order for the simulation to produce reliable results, it is essential that certain guidelines are followed concerning mainly the spacing and time resolution of the wave equation solution. The spacing resolution, was set to 3 mm which is less than one tenth of the excited wavelength (approximately 47 mm for frequency of 100 kHz), while the sampling time was 0.193 μs, much less than the period of the excited wave (10 μs), enabling each cycle to be represented by approximately 50 points, while 20 points are considered satisfactory.[27] The geometry of the model is seen in Figure 2. It represents a 2 m long concrete beam with a width of 0.4 m. Concrete was modeled as a matrix containing aggregates of 20 mm diameter in a percentage of 34% by cross section area. Apart from the case of intact concrete which was simulated initially, different cases of crack densities were examined. Cracks were simulated by thin films of dimensions 20x3 mm. Three different orientations were applied, namely 90°, 45° and −45° with respect to the horizontal axis. The horizontal and vertical spacing for the cracks of each orientation was 50 mm for 5.7% content (as measured by cross-section area). The cases 2.8% and 1.4% were also simulated. Initially, the displacement excitation was conducted at the lower left end of the model with a direction to the right (see Figure 2 top). It was one cycle of 10 μs duration (main frequency 100 kHz), while later 200 kHz were also applied. The 'receivers' were placed on the top surface of the geometry, with a separation distance of 300 mm and provided the average vertical displacement over their length, meaning that each receiver's signal represents the average response over a number of nodes. At the right and left ends of the beam, infinite boundary conditions were applied in order to avoid reflections and resembled a beam much longer than the measurement area.

Results

The snapshots of the displacement field in Figure 2 show the wave spreading away from the point source at three distinct moments after excitation. As the wave front propagates, it reaches the adjacent transducers and the transient responses of the sensors are recorded. The waveforms obtained by the seven receivers are seen in Figure 3 for the cases of intact concrete (elastic matrix with stiff aggregates, case a) and heavily cracked concrete (elastic matrix with aggregates and 5.7% randomly oriented cracks, case b). It is mentioned that contrary to the experimental amplitude, that is eventually measured in Volts due to piezoelectric transformation in the sensors, the amplitude of the simulation is non dimensionless.

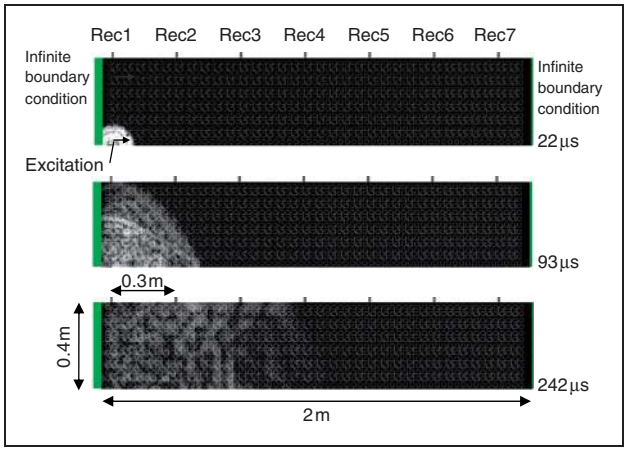

Figure 2. Geometric model and consecutive snapshots of the displacement field.

Table 1. Properties of materials used in the numerical model

	λ (GPa)	μ (GPa)	η (Pa·s)	ξ (Pa·s)	ρ (kg/m^3)	C_P (m/s)
Mortar Matrix	11.1	16.6	2500	$3.26*10^{-4}$	2300	4735
Aggregates	14.3	25.4	2500	$3.26*10^{-4}$	2600	5190
Cracks	10^{-4}	10^{-6}	–	–	1.2	300

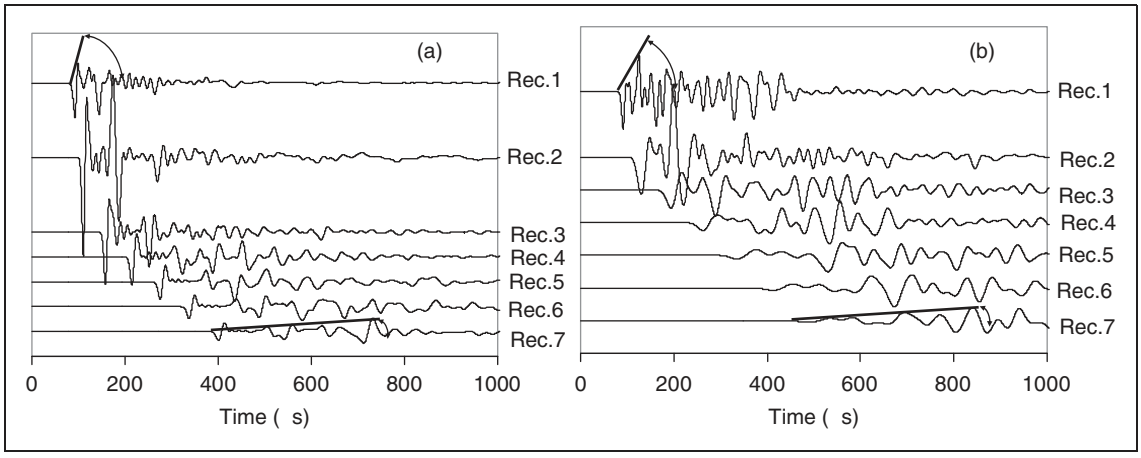

Figure 3. Simulated waveforms collected at different sensors for (a) intact concrete and (b) concrete with 5.7% cracks.

Apart from the delay imposed to the waveform of the consecutive transducers, there is also a strong influence on the shape of the pulse. Specifically, receiver 1 which is placed above the excitation, records a signal with short RT, which reaches its maximum shortly after the onset and consecutively exhibits small RA. However, as the distance increases, the rise angle of the waveform decreases and the maximum amplitude delays more relatively to the onset, as seen for Receiver #7 in Figure 3(a). The waveform shapes change even more for the case of Figure 3(b) that concerns concrete with 5.7% cracks. It is characteristic that the first cycle of the recorded waveforms is much less sharp for the cracked material compared to the intact one, due to the scattering of the wave front. For the case of 5.7% cracks, the waveforms of receivers 1 and 7 are separately depicted in Figure 4, along with their basic calculated parameters. Apart from the amplitude difference, which is expected due to damping, scattering, and wave front spreading, the total number of threshold crossings is lower for the far away receiver, leading to lower AF, while the maximum peak delays relatively to the onset leading to a longer RT of 323 μs, as compared to the 29 μs of the closer receiver. Concerning RA, its value increases by more than 30 times for the furthest receiver, highlighting that the same source event is captured in a very different way at different positions. It is mentioned that the threshold is constant for all waveforms and was set equal to 1/100 of the highest peak exhibited by any of the signals, which is a realistic value.

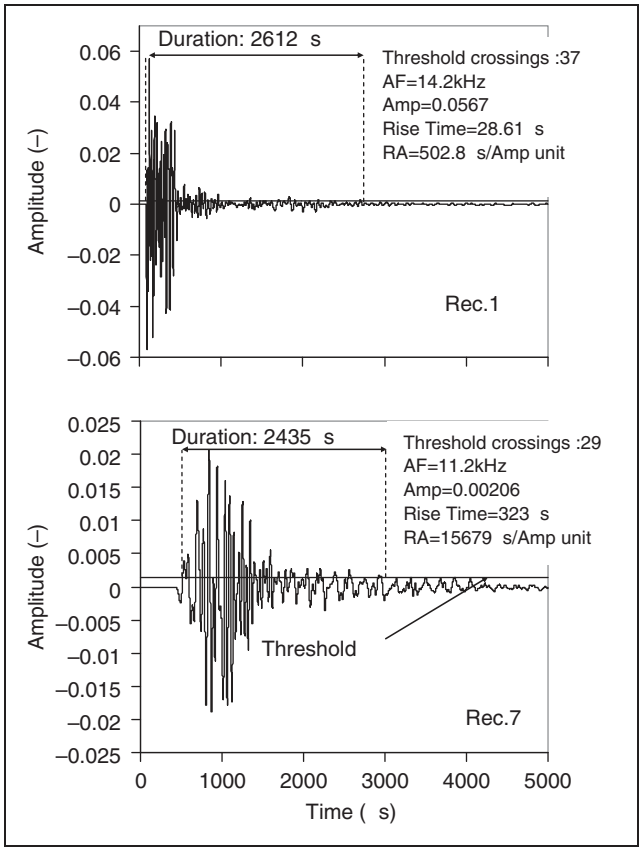

Figure 4. Whole waveforms of Rec. 1 and 7 from Figure 4(b). The dashed lines denote the first and last threshold crossings.

By calculating the specific waveform parameters that are of interest for AE one can draw valuable conclusions for their dependence on propagation distance. Figure 5(a) shows the RA values calculated for the different receivers (1-7), as a function of the horizontal distance from the source and the different material conditions. It can be seen that for the case of plain concrete, the RA stays approximately constant up to the distance of 1.5 m, but becomes unstable at 1.8 m. This change in the RA of the pulse is evident at closer distances if the material contains cracks, something reasonable due to the increased scattering dispersion. For the case of cracks at a percentage of 1.4%, the RA increases for distances longer than 0.9 m, while for cracks at 5.7%, the RA becomes unstable at distances longer than 0.6 m.

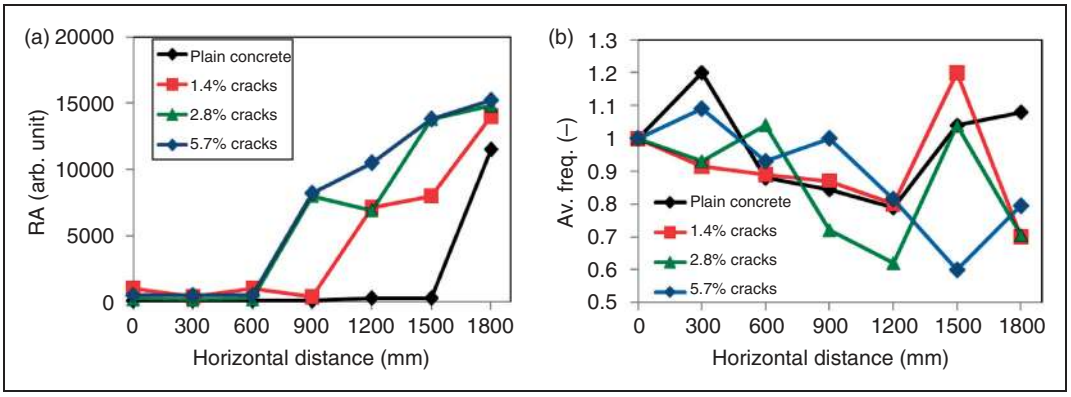

Figure 5. Simulated results of (a) RA and (b) AF vs horizontal distance between excitation and receivers.

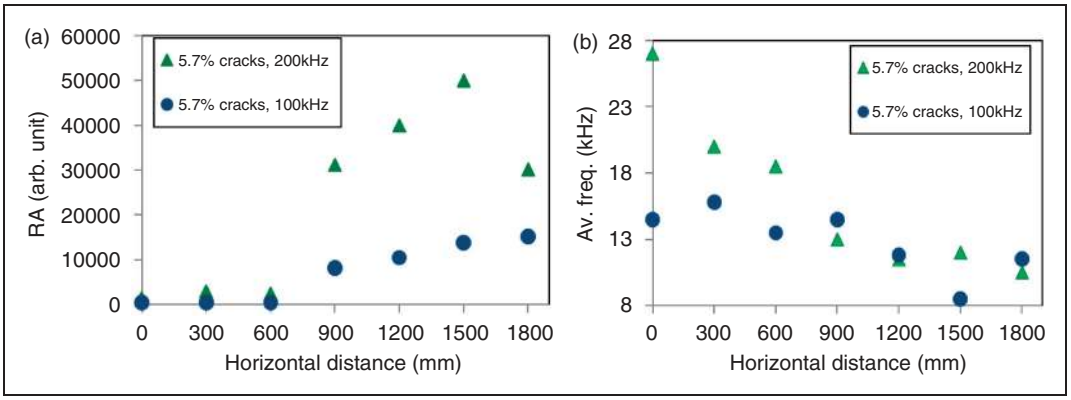

Figure 6. Simulated results of (a) RA and (b) AF vs horizontal distance between excitation and receivers for different frequencies.

Therefore, it can be concluded that both propagation distance and material condition strongly influence the shape of the pulse.

Figure 5(b) shows the behavior of AF (number of threshold crossings over signal duration) as a function of distance for different material conditions. Despite some fluctuations, there is a decreasing trend of AF with distance reaching approximately a value even 40% lower than the nearest sensor. This decrease is crucial since it can mask the frequency decrease due to the shift of the mechanisms during actual fracture, as will be discussed below.

Influence of excitation frequency

In case the initial pulse is one cycle of 200 kHz, the results can be seen in Figure 6(a) and (b) concerning RA and AF respectively along with the results of 100 kHz which are supplied for comparison. Concerning RA it is obvious that for both frequencies, consistent measurements are conducted up to the distance of 600 mm, while for longer distances the resulted RA is more than one order of magnitude higher. This numerical result implies that there is a threshold distance (between 600 mm and 900 mm) above which the measurements lead to inconsistent values. The situation is similar for AF, since even for an excitation frequency of 200 kHz, the measured AF, decreases strongly. For a horizontal distance of 900 mm (Rec. 4) the AF is approximately the same as that of 100 kHz pulse, exhibiting a decrease of more than 50% compared to Rec. 1. This highlights the severity of scattering on the aggregates and cracks. It is clear that the frequency content of the pulse, as measured by the oscillations of the signal within the specified duration, reveals a decrease of 90% (AF is approximately 20 kHz or less) compared to the excited frequency, showing that the material inhomogeneity acts as a low-pass filter.

Influence of orientation and wave type

The above mentioned cases were simulated with the excitation at the left bottom of the model, while the transient displacement direction was horizontal (see top of Figure 2). In order to test a few more indicative possibilities, the simulations were repeated with some changes in the excitation. Specifically, with the same position (bottom left of the model, in Figure 2, snapshot at 22 μs), the excitation direction was set upwards. Additionally, in another case, the original direction was used but the pulse was

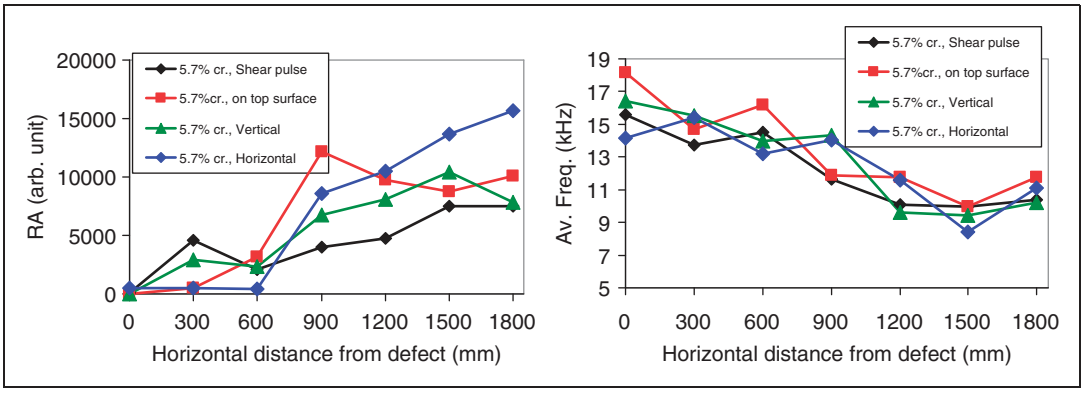

Figure 7. Simulated results of (a) RA and (b) AF vs horizontal distance between excitation and receivers for different excitations.

excited on the top surface (near Rec. 1). The final case was similar to the original configuration but instead of longitudinal excitation, shear pulse was applied. Results concerning the RA and AF are depicted in Figure 7(a) and (b). It is suggested that propagation longer than 600 mm in cracked concrete results in much higher RA values compared to propagation up to 600 mm. The shear pulse can be regarded as an exception, because it exhibits high RA value even for 300 mm. The AF, which is presented in Figure 7(b), shows a consistent drop as the distance becomes longer. For 1.5 m, the AF has dropped by 50% for any type of excitation in damaged concrete.

Discussion

Before discussing the specific trends as measured by the simulations, it should be highlighted that this study focuses on the propagation of the pulse through the medium and not on the emission from the crack itself. Thus the applied excitation of one cycle is indicative and not directly connected to the actual excitation imposed by the crack tip motion. The focus is given on the combined effect of aggregates and cracks on the distortion of the elastic wave. The effect of a single crack on propagation is quite clear in wave propagation studies, modifying the frequency, amplitude, and velocity readings.[28,29] When a population of randomly oriented cracks is present (which is the case for damaged concrete) their effect is cumulative and the characteristics of a propagating pulse are completely changed compared to the initial.[20,30] Aggregates also influence the propagation; however their density and wave velocity is quite similar to the mortar matrix, resulting in weak scattering of the wavefront; on the other hand cracks, which exhibit a density and wave velocity near zero are much stronger scatterers of elastic waves when inside a stiff elastic matrix.

From the above results, it is seen that waveform parameters used for crack classification, like RA and AF although may depend on the mode of the source crack, can be severely influenced by long propagation through damaged material. This practically means that a specific tensile event recorded by a transducer nearby the crack in intact concrete will be characterized as mode I, while if the material is deteriorated and the receiver is placed away from the source, the same event would more likely be characterized as mode II. This dependence of RA on the material and testing parameters is crucial. From Figure 5(a), it can be seen that for distances within 600 mm, the RA is contained between 50 and 1000, while for longer distances it increases above 6000. Therefore, the distance in combination to the material's condition may lead to an increase of the calculated RA by 6 to 100 times, meaning that this change would more likely mask the actual source, falsely shifting the characterization in favor of the mode II. It is highlighted that the actual change of RA based on the cracking type alone as was measured experimentally for SFRC, was of the order of 4–10. Specifically, the RA of tensile cracking was less than 500 μs/V, while later when shear was active it increased to about 2000 μs/V.[13,14] Therefore, a change by 10 or more times due to distance would mask the effect of the crack type itself.

As to the AF, again the change due to long propagation in damaged material may mask the effect of the source crack type. The decrease of AF, unlike RA, is gradual and does not become suddenly unstable after a certain distance. Simulation results presented in Figures 5(b), 6(b) and 7(b) show a decrease of approximately 50% in the AF of a signal propagating through 1.5 M or 1.8 m of concrete.This decrease is crucial since the AF decrease caused by different failure mechanisms (matrix cracking and fibre pull-out) as measured experimentally is of the same order. Specifically, AF decreased from 300 to 150 kHz after main failure, being reduced by 50%.[13,14] However, this study shows that 1 m propagation away from the source could result in decrease similar to that imposed by the shift of failure mechanisms.

The above discussion raises a crucial subject concerning AE monitoring of large structures. It can be

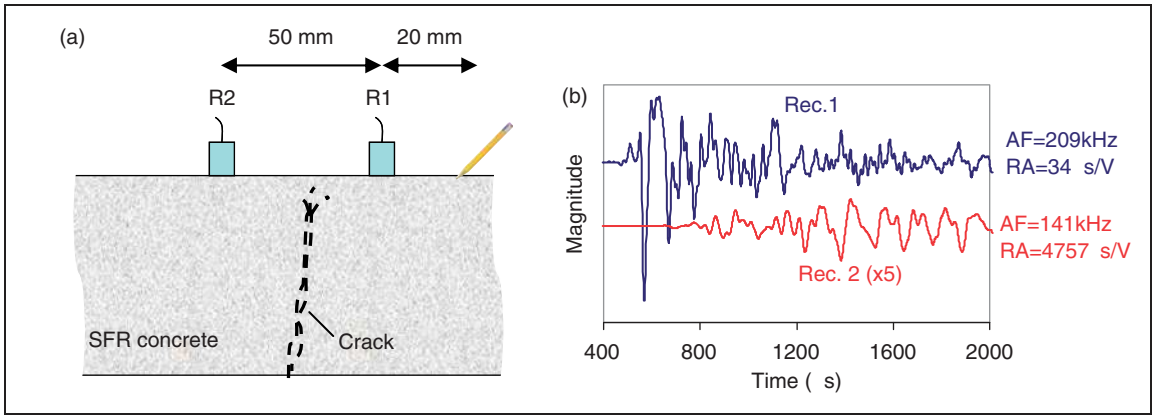

Figure 8. (a) Schematic representation of surface wave measurements in cracked concrete and (b) waveforms of the two receivers, with the basic AE parameters.

concluded that the specific values of the different indices should always be connected to the propagation distance. Alternatively, in order to characterize the cracking mode, data should be collected by sensors at close distances around the source event, while events located away should not be considered for this purpose. The present simulations imply a propagation distance of 600 mm, within which, the indices measurements is consistent for any type of material. It is interesting to examine the above considerations in actual AE experiments with different type of concrete, concerning its aggregate content and size in order to propose a robust classification scheme with the minimum possible influence of distance.

Apparently, the above discussion does not include the deterministic aspects of AE, like event location, which are not influenced by the shape of the waveform, but only from the arrival time of the signal. In practical terms, location of the cracking zones may be conducted even for long distances between the AE sensors, but when detailed assessment of the failure mode is attempted, the receivers should be quite close, or events located far from the receivers should be excluded from crack classification analysis.

As an indicative example of the experimental behavior of the pulses in damaged material the following case is presented. The material was SFRC, which had been tested in bending and developed a deep network of cracks. The excitation was conducted with a pencil lead fracture on the surface of the specimen, as seen in Figure 8, which is received by two broad band sensors at distances of 20 m and 70 mm. The waveforms received at both positions are seen in Figure 8(b) with some of their main characteristics. The AF dropped from 209 kHz at the near-by sensor to 141 kHz after additional 50 mm of propagation, while for the same distance the RA increased by 140 times (4757 μs/vs. over 34 μs/V). This example is indicative of the influence of the propagation distance on AE parameters in cracked material. A specific initial excitation (in this case fracture of pencil lead) would be classified as mode I by Rec. 1, due to low RA and high AF, while it would be classified as mode II by the Rec. 2.

Conclusion

The present article deals with the dependence of AE parameters to the propagation distance and the quality of the propagation path. Numerical simulations show that crucial indices like the AF and the RA are strongly influenced, masking therefore, the source information contained in the initial pulse. The source itself may be responsible for a decrease of 50% in frequency, which is approximately the percentage of decrease imposed by longer propagation in cracked material. Additionally, as recent experiments have shown, the RA value may increase by about 4 to 10 times for a shear crack, relatively to a tensile one, but long propagation through concrete may impose a much higher increase of the order of 30 times or more. It is obvious that the combined effect of attenuation and dispersion exercises have strong influence on the AE parameters value. This should be seriously taken into account before applying crack classification approaches in concrete structures and specimens. Additionally, further study is necessary, in order to include results in specific recommendations concerning the separation distance of AE sensors for characterization of cracks in concrete. As a future step, AE monitoring during fracture experiments of mortar specimens with a notch is scheduled. The notch will serve as crack initiator and the parameters of the AE signals captured by sensors at different distances from the notch will allow experimental correlations between the propagation distance and AE parameters.

Funding

This research received no specific grant from any funding agency in the public, commercial, or not-for-profit sectors.

References

1. Grosse CU and Ohtsu M. *Acoustic emission testing*. Heidelberg: Springer, 2008.
2. Mindess S. Acoustic emission methods. In: Malhotra VM and Carino NJ (eds) *CRC handbook of nondestructive testing of concrete*. Boca Raton, FL: CRC Press, 2004.
3. Kurz JH, Finck F, Grosse CU and Reinhardt HW. Stress drop and stress redistribution in concrete quantified over time by the B-value analysis. *Struct Health Monit* 2006; 5(1): 69–81.
4. Lovejoy SC. Acoustic emission testing of beams to simulate SHM of vintage reinforced concrete deck girder highway bridges. *Struct Health Monit* 2008; 7(4): 329–346.
5. Aggelis DG, Shiotani T, Momoki S and Hirama A. Acoustic emission and ultrasound for damage characterization of concrete elements. *ACI Mater J* 2009; 106(6): 509–514.
6. Grosse C, Reinhardt H and Dahm T. Localization and classification of fracture types in concrete with quantitative acoustic emission measurement techniques. *NDT & E Int* 1997; 30(4): 223–230.
7. Anastassopoulos AA and Philippidis TP. Clustering methodology for evaluation of acoustic emission from composites. *J Acoust Emiss* 1995; 13(1/2): 11–22.
8. Ohtsu M and Tomoda Y. Phenomenological model of corrosion process in reinforced concrete identified by acoustic emission. *ACI Mater J* 2007; 105(2): 194–200.
9. Shiotani T, Ohtsu M and Ikeda K. Detection and evaluation of AE waves due to rock deformation. *Constr Build Mater* 2001; 15(5-6): 235–246.
10. Aggelis DG, Matikas TE and Shiotani T. Advanced acoustic techniques for health monitoring of concrete structures. In: Kim SH and Ann KY (eds) *The Song's handbook of concrete durability*. Seoul, Korea: Middleton Publishing Inc, 2010, pp. 331–378.
11. RILEM Technical Committee. (2010). Recommendation of RILEM TC 212-ACD: acoustic emission and related NDE techniques for crack detection and damage evaluation in concrete, test method for classification of active cracks in concrete structures by acoustic emission. *Mater Struct* 2010; 43(9): 1187–1189.
12. Aggelis DG, Barkoula NM, Matikas TE and Paipetis AS. Acoustic emission monitoring of degradation of cross ply laminates. *J Acoust Soc Am* 2010; 127(6): EL246–251.
13. Aggelis DG, Soulioti DV, Sapouridis N, Barkoula NM, Paipetis AS and Matikas TE. Characterization of the damage process in fibre reinforced concrete using acoustic emission parameters. In: *Proceedings of 4th International Conference on Structural Faults & Repair-2010, 15–17 June*, Edinburgh, UK, 2010 (in CD).
14. Soulioti D, Barkoula NM, Paipetis A, Matikas TE, Shiotani T and Aggelis DG. Acoustic emission behaviour of steel fiber reinforced concrete under bending. *Constr Build Mater* 2009; 23(12): 3532–3536.
15. Lu Y, Li Z and Liao WI. Damage monitoring of reinforced concrete frames under seismic loading using cement-based piezoelectric sensor. *Mater Struct* 2010; 44(7): 1273–1285. DOI: 10.1617/s11527-010-9699-0.
16. Verbis JT, Kattis SE, Tsinopoulos SV and Polyzos D. Wave dispersion and attenuation in fiber composites. *Comput Mech* 2001; 27(3): 244–252.
17. Aggelis DG and Philippidis TP. Ultrasonic wave dispersion and attenuation in fresh mortar. *NDT & E Int* 2004; 37(8): 617–631.
18. Cowan ML, Beaty K, Page JH, Zhengyou L and Sheng P. Group velocity of acoustic waves in strongly scattering media: Dependence on the volume fraction of scatterers. *Phys Rev E* 1998; 58(5): 6626–6636.
19. Aggelis DG, Tsinopoulos SV and Polyzos D. An iterative effective medium approximation (IEMA) for wave dispersion and attenuation predictions in particulate composites, suspensions and emulsions. *J Acoust Soc Am* 2004; 116(6): 3443–3452.
20. Aggelis DG. Numerical simulation of wave propagation in material with inhomogeneity: inclusion size effect. *NDT & E Int* 2009; 42(6): 558–563.
21. Surgeon M and Wevers M. Modal analysis of acoustic emission signals from CFRP laminates. *NDT & E Int* 1999; 32(6): 311–322.
22. Prosser WH. The propagation characteristics of the plate modes of acoustic emission waves in thin aluminum plates and thin graphite/epoxy composite plates and tubes. *J Acoust Soc Am* 1992; 92: 3441–3442.
23. RILEM Technical Committee MCM, 2010. 'On-Site Measurement of Concrete and Masonry Structures by Visualized NDT', *Online Referencing,* http://www.rilem.net/tcDetails.php?tc=MCM (2010, accessed July 2011).
24. Wave 2000. 'Cyber-Logic, Inc, NY', *Online Referencing,* http://www.cyberlogic.org (2000, accessed July 2011).
25. Kaufman JJ, Luo G and Siffert RS. Ultrasound simulation in bone. *IEEE T Ultrason Ferr* 2008; 55(6): 1205–1218.
26. Aggelis DG and Shiotani T. Experimental study of surface wave propagation in strongly heterogeneous media. *J Acoust Soc Am* 2007; 122(5): EL151–157.
27. Moser F, Jacobs LJ and Qu J. Modeling elastic wave propagation in waveguides with finite element method. *NDT & E Int* 1999; 32(4): 225–234.
28. Aggelis DG, Shiotani T and Polyzos D. Characterization of surface crack depth and repair evaluation using Rayleigh waves. *Cement Concrete Comp* 2009; 31(1): 77–83.
29. Pecorari C. (2001). Scattering of a Rayleigh wave by a surface-breaking crack with faces in partial contact. *Wave Motion* 2001; 33(3): 259–270.
30. Aggelis DG and Shiotani T. Experimental study of surface wave propagation in strongly heterogeneous media. *J Acoust Soc Am* 2007; 122(5): EL151–157.